Received: 30 July 2024 | Revised: 21 February 2025 | Accepted: 27 February 2025

DOI: 10.1002/ijc.35409

RESEARCH ARTICLE

Cancer Therapy and Prevention

IJC INTERNATIONAL JOURNAL of CANCER | UICC

Antitumor efficacy of intermittent low-dose erlotinib plus sulindac via MHC upregulation and remodeling of the immune cell niche

Chakrapani Tripathi[1] | Jorge E. Tovar Perez[1] | Sabeeta Kapoor[1] | Ahmed Muhsin[1] | Wan Mohaiza Dashwood[1] | Yunus Demirhan[1] | Melek Demirhan[1] | Alessandro Shapiro[1] | Altaf Mohammed[2] | Shizuko Sei[2] | Jacklyn Thompson[3] | Mahira Zaheer[3] | Krishna M. Sinha[3] | Powel H. Brown[3] | Michelle I. Savage[3] | Eduardo Vilar[3] | Praveen Rajendran[1] | Roderick H. Dashwood[1]

[1]Center for Epigenetics & Disease Prevention, Texas A&M HEALTH, and Department of Translational Medical Sciences, Texas A&M University Naresh K. Vashisht College of Medicine, Houston, Texas, USA

[2]Chemopreventive Agent Development Research Group, Division of Cancer Prevention, National Cancer Institute, Rockville, Maryland, USA

[3]Department of Clinical Cancer Prevention, The University of Texas MD Anderson Cancer Center, Houston, Texas, USA

Correspondence
Roderick H. Dashwood and Praveen Rajendran, Center for Epigenetics & Disease Prevention, Texas A&M HEALTH, 2121 W. Holcombe Blvd., Houston, TX 77030, USA.
Email: rdashwood@tamu.edu; prajendran@tamu.edu

Funding information
Division of Cancer Prevention, National Cancer Institute, Grant/Award Numbers: P30 CA016672, RO1 CA122959, RO1 CA257559, T.O. 75N91019D00021, T.O. 75N91019F00130

Abstract

A previously reported clinical trial in familial adenomatous polyposis (FAP) patients treated with erlotinib plus sulindac (ERL + SUL) highlighted immune response/interferon-γ signaling as a key pathway. In this study, we combine intermittent low-dose ERL ± SUL treatment in the polyposis in rat colon (Pirc) model with mechanistic studies on tumor-associated immune modulation. At clinically relevant doses, short-term (16 weeks) and long-term (46 weeks) ERL ± SUL administration results in near-complete tumor suppression in Pirc colon and duodenum ($p < 0.0001$). We identify a low-dose threshold for significant antitumor activity in Pirc rats given SUL at 125 ppm in the diet plus ERL at 5 mg/kg body weight via twice-weekly oral gavage (SUL125 + ERL5 × 2). Longitudinal analyses show diminished expression of MHC class I and II genes in polyps larger than Grade 5, a novel finding in the Pirc model. Treatment with ERL ± SUL upregulates the corresponding MHC and immune-associated factors in a subset of Pirc colon polyps, Pirc tumor cell lines, murine colon carcinoma cells, and FAP patient-derived organoids, with Nlrc5 playing a critical role in this effect. Imaging mass cytometry reveals that SUL125 + ERL5 × 2 increases tumor-associated $Cd4^+$ T cells by ~2.6-fold ($p < 0.05$), with no apparent effect on $Cd8^+$ T cells. The treatment also increases tumor-associated $Cd68^+$ cells ($p < 0.05$) and decreases $Foxp3^+$ ($p < 0.01$) and $Arg1^+$ ($p < 0.05$) cells. Thus, intermittent low-

Abbreviations: ERL, erlotinib; FAP, familial adenomatous polyposis; GrB, granzyme B; IFN-γ, interferon-γ; IHC, immunohistochemistry; IMC, imaging Mass Cytometry; MHC, major Histocompatibility Complex; NSAIDs, nonsteroidal anti-inflammatory drugs; PCT, Pirc colon tumor; PDT, Pirc duodenal tumor; pErk, phosphorylated extracellular signal-regulated kinase; Pirc, polyposis in rat colon; SUL, sulindac.

Chakrapani Tripathi, Jorge E. Tovar Perez, and Sabeeta Kapoor contributed equally to this study and are listed as co-first authors.

dose ERL + SUL treatment enhances tumor-associated MHC expression and remodels the immune cell niche toward a more permissive "helper" immune microenvironment. We conclude that early immune-interception strategies targeting interferon-γ signaling may benefit FAP patients at drug doses below the clinical standard of care.

KEYWORDS
erlotinib, familial adenomatous polyposis (FAP), MHC, sulindac, tumor immunomodulation

What's New?

Novel immunomodulatory insights derived from experimental models and clinical samples reveal the cancer-preventive potential of intermittent low-dose erlotinib plus sulindac (ERL + SUL). This study shows that ERL + SUL treatment upregulates MHC class I and II expression and remodels the immune cell niche, with significant tumor suppression observed in the Pirc model that closely mimics clinical FAP. These findings suggest a promising strategy for human cancer prevention at potentially safe doses. These results highlight the potential for success in clinical trials, emphasizing early combinatorial immune-interception targeting interferon-γ signaling.

1 | INTRODUCTION

Familial adenomatous polyposis (FAP) is a hereditary condition characterized by numerous adenomatous polyps in the gut, requiring prophylactic colectomy as well as anticancer interventions.[1–3] Nonsteroidal anti-inflammatory drugs (NSAIDs) suppress adenomatous polyps in the colon, but not without resistance and/or toxicity, and have lower efficacy in the duodenum, where tumor formation also is of concern.[2,3] A clinical trial in FAP patients demonstrated that sulindac plus erlotinib (SUL + ERL) had efficacy in the duodenum and colon,[4,5] but dose modification was recommended to reduce skin toxicity associated with ERL treatment. Subsequent dose-response, time-course, and pharmacodynamic studies in the polyposis in rat colon (Pirc) model[6] revealed significant antitumor activity in the colon and duodenum after SUL ± ERL treatment.[7] Tumor suppression was particularly effective for rats ingesting 250 parts per million (ppm) SUL in the diet, equivalent to the SUL standard of care, combined with intragastric (*i.g.*) ERL administration at 10, 21, or 42 mg/kg body wt. (BW), that is, one-quarter, one-half, or the clinical-equivalent dose of ERL, given once a week rather than daily.[7] Once-a-week ERL dosing in the rat predicted efficacy outcomes in a subsequent trial in FAP patients,[8] highlighting the clinical translatability of the Pirc model.

Prior intermittent dosing experiments with ERL used phosphorylated extracellular signal-regulated kinase (pErk) as a biomarker of drug efficacy.[9] However, in Pirc tumors at 1 year, the extent of pErk inhibition did not parallel the dose-dependent antitumor outcomes observed following long-term SUL±ERL treatment.[7] We sought additional mechanistic leads from transcriptomic data in FAP patients given SUL+ERL versus placebo,[10] which prioritized WNT, EGFR, and COX/PGE2 pathways, as well as immune response/interferon-γ (IFN-γ) genes.[10] The latter findings support an evolving new paradigm for the immune microenvironment in FAP.[11]

The current investigation builds upon our prior research, focusing for the first time on the timing of IFN-γ signaling changes in tumors from the Pirc model, while conducting additional SUL + ERL dose-titration experiments.[10] We report here on the temporal changes in Major Histocompatibility Complex (MHC) class I and II gene expression in Pirc tumors and the immunomodulatory mechanisms of low-dose SUL + ERL combinations in vivo, with additional corroboration in cell-based assays and FAP patient-derived organoids. The strategy of examining SUL±ERL at low-dose combinations seeks to mitigate reported drug toxicities in the clinical setting,[2,3] while exploring the potential for modulation of the tumor microenvironment with a view to early immune interception.

2 | MATERIALS AND METHODS

2.1 | Preclinical studies

Following an approved IACUC protocol (2023-0087-H), rats were maintained in AAALAC-certified facilities by crossing F344/NTac *Apc*$^{Pirc/+}$ males and F344 females under a Taconic Breeding Agreement (Taconic, Hudson, NY). Studies involving experiments with animals and their care were conducted in accordance with institutional guidelines. Ear punches were used for identification and genotyping.[6] Food consumption and BW were recorded weekly. Water and basal AIN93 or custom diets (Research Diets, NJ) were provided ad libitum. Based on a recent report,[7] SUL (>98% purity, catalog #S8139, Lot #MKCH7987, Millipore Sigma, St. Louis, MO) was fed in AIN93 diet, whereas ERL (>99% purity, catalog #E-4007, Lot #BBE-108, LC Laboratories, Woburn, MA) was given via intragastric (*i.g.*) oral gavage, formulated immediately before dosing in sterile 30% Captisol®. Littermates were randomized to treatments, and no water or food aversion was observed based on weekly intake records.

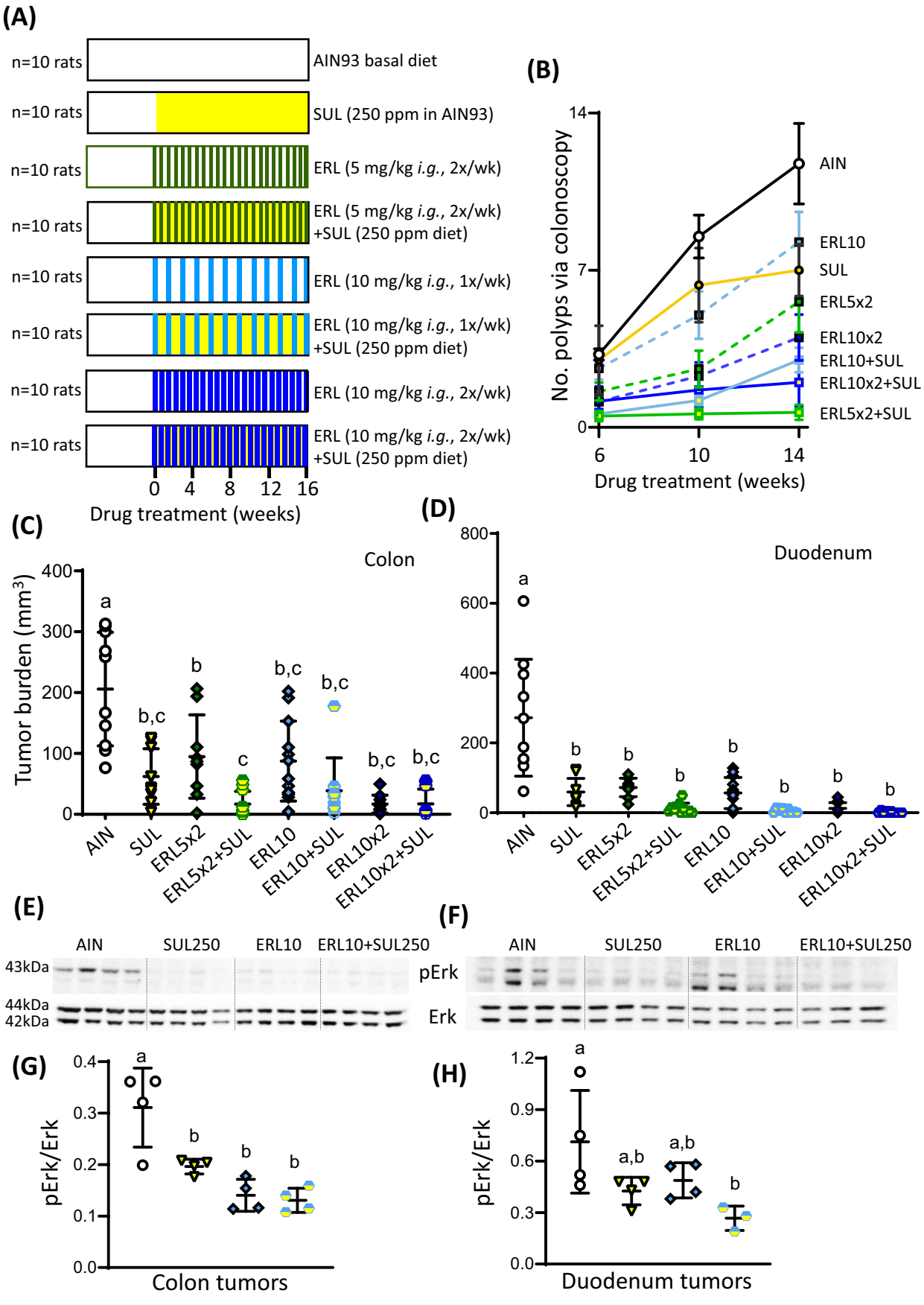

FIGURE 1 Legend on next page.

2.2 | Dosing protocols

A short-term study involving 16 weeks of SUL ± ERL treatment was followed by a long-term investigation lasting 1 year, in which rats received test agents for a total of 46 weeks.[7] Power calculations and group sizes were based on a prior report,[7] with rats assigned randomly to each treatment group.[7] In the short-term study (Figure 1), at 6 weeks of age, Pirc males were fed an AIN93 basal diet or switched to an AIN93 diet containing 250 ppm SUL, which equates to the standard of care SUL in FAP patients taking 150 mg of the drug twice daily.[4] Based on our prior report,[7] rats received SUL alone or in combination with ERL via *i.g.* oral gavage. Once-a-week ERL at 10 mg/kg BW is equivalent to 125 mg in humans, or one-quarter of the weekly intake of ERL given at 75 mg daily in FAP patients.[4] Other groups received 5 or 10 mg/kg BW ERL twice per week, alone or in combination with SUL. The number of polyps visible by screening colonoscopy[12] was recorded in each animal at 6, 10, and 14 weeks of drug treatment, and 2 weeks later, the study was terminated. Tissues were harvested for molecular studies, as reported.[7]

In the long-term investigation (Figure 2), at 6 weeks of age, Pirc males were fed AIN93 diet or switched to AIN93 diet containing 125 or 250 ppm SUL, given continuously or on alternating weeks, respectively. Treatment with SUL equated to one-half of the clinical standard of care over the course of the dosing schedule. Other groups received *i.g.* intubation of ERL at 5 or 10 mg/kg BW twice per week, alone or in combination with SUL. Test agents were administered for a total of 46 weeks, at which point the study was terminated, that is, in rats aged 1 year. Polyp size was measured using vernier calipers at necropsy. Tumor volume was calculated as length $\times$ width^2 $\times$ 0.5, and the total tumor burden was determined by summing the individual volumes of all polyps. Grading was performed using a previously established methodology that is based on tumor volume.[7,12] Tissues were harvested for molecular and drug safety assessment, and also for immunohistochemistry (IHC) analyses, as reported.[7,13–16]

2.3 | RNA assays

Frozen tumors and normal tissues were thawed for RNA extraction, as reported.[13–16] RNA (2 µg) was reverse-transcribed in 20 µL using the SuperScript® III first-strand synthesis system (Invitrogen). Target mRNAs were quantified by qPCR. Forty cycles of PCR (95°C/10 s, 58°C/10 s, 72°C/10 s) were run on a LightCycler 480 II system (Roche, Indianapolis), in a 20-µL total reaction volume containing cDNAs, SYBR Green I dye (Roche), and gene-specific primers for rat *B2m*, *Cnx*, *Psmb8*, *RT1-A2*, *Tap1*, *Cd74*, *RT-1Bb*, *Cd4*, and *Ciita*. The amount of specific mRNA was quantified from the Ct ratio of the target gene to *glyceraldehyde-3-phosphate dehydrogenase (Gapdh)*. At least three experiments were performed for each sample, with nine tumors per group.

2.4 | Immunoblotting and IHC

Proteins (20 µg) were subjected to SDS-PAGE and immunoblotting (IB) analyses according to reported methodologies.[7,13–16] Primary antibodies were to CD163 (ABclonal #A8383, 1:1000), pErk (Sigma-Aldrich #05–797, 1:2000), Erk (Cell Signaling Technology #9107, 1:1000), β-catenin (Cell Signaling Technology #9581, 1:1000), Cox2 (Cell Signaling Technology #12282, 1:500), Tnfα (R&D system #MAB510, 1:1000), Il-1β (R&D system #MAB5011, 1:1000), Mmp7 (Cell Signaling Technology #3801, 1:1000), Nlrc5 (Invitrogen #PA5-21017, 1:1000), B2m (Invitrogen #PA5-88527, 1:1000), Psmb8 (Proteintech #14859-1-AP, 1:1000), Psmb9 (Invitrogen #MA5-35805, 1:1000), poly(ADP-ribose) polymerase (PARP) (Cell Signaling Technology #9542S, 1:1000), Tap1 (Proteintech #11114-1-AP, 1:1000), MHC-I anti-rat RT1.A (Invitrogen #MA1-70005, 1:500), pan-MHC-I anti-mouse (Invitrogen #PA5-115364, 1:1000) and β-actin (Sigma-Aldrich #A1978, 1:4000). Proteins were visualized by Western Lightning Chemiluminescence Reagent Plus and quantified as reported.[13]

Protein expression of B2m in Pirc colon tumors also was determined by IHC (The University of Texas MD Anderson Cancer Center, DVMS Veterinary Pathology Services Core, Houston, TX). Tissues were fixed in 10% formalin, embedded in paraffin, and 4–5 µm sections were mounted on glass slides. Following deparaffinization and rehydration through standard procedures,[14] antigen retrieval was performed in citrate buffer for 20 min at a 1:5000 dilution. Sections were incubated with primary antibody specific to rat B2m (Invitrogen # PA5-29580) for 60 min, followed by secondary antibody for 30 min at room temperature in the dark. After washing in PBS, slides were coated with chromogenic substrate 3,3'-diaminobenzidine for 5 min and counterstained with hematoxylin for 30–60 s. Slides were washed in water and then immersed in graded ethanol solutions and xylene for rehydration,[14] followed by examination under the microscope.

2.5 | Imaging Mass Cytometry (IMC)

Pirc colon tumors were harvested during necropsy and promptly embedded in optimal cutting temperature (OCT) medium (Sakura

FIGURE 1 Short-term intermittent low-dose ERL ± SUL treatment suppressed tumor formation in the colon and duodenum of the Pirc model and reduced pErk expression. (A) Short-term efficacy protocol involving 16-week dosing of test agents. (B) Temporal tracking of antitumor response by colonoscopy (mean ± SE). (C, D) Scatter plots of antitumor activity in the colon and duodenum, respectively, at 16 weeks, with each animal represented by a single datapoint; horizontal line, median. (E, F) Representative immunoblots of pErk and Erk in Pirc colon and duodenum tumors, respectively, at 16 weeks. Each lane represents an individual polyp, and the data are representative of three or more independent experiments. In panels (G, H) immunoblots were quantified from Pirc colon and duodenum tumors, respectively, and groups sharing the same superscript letter were not significantly different by one way ANOVA (GraphPad Prism 9.5).

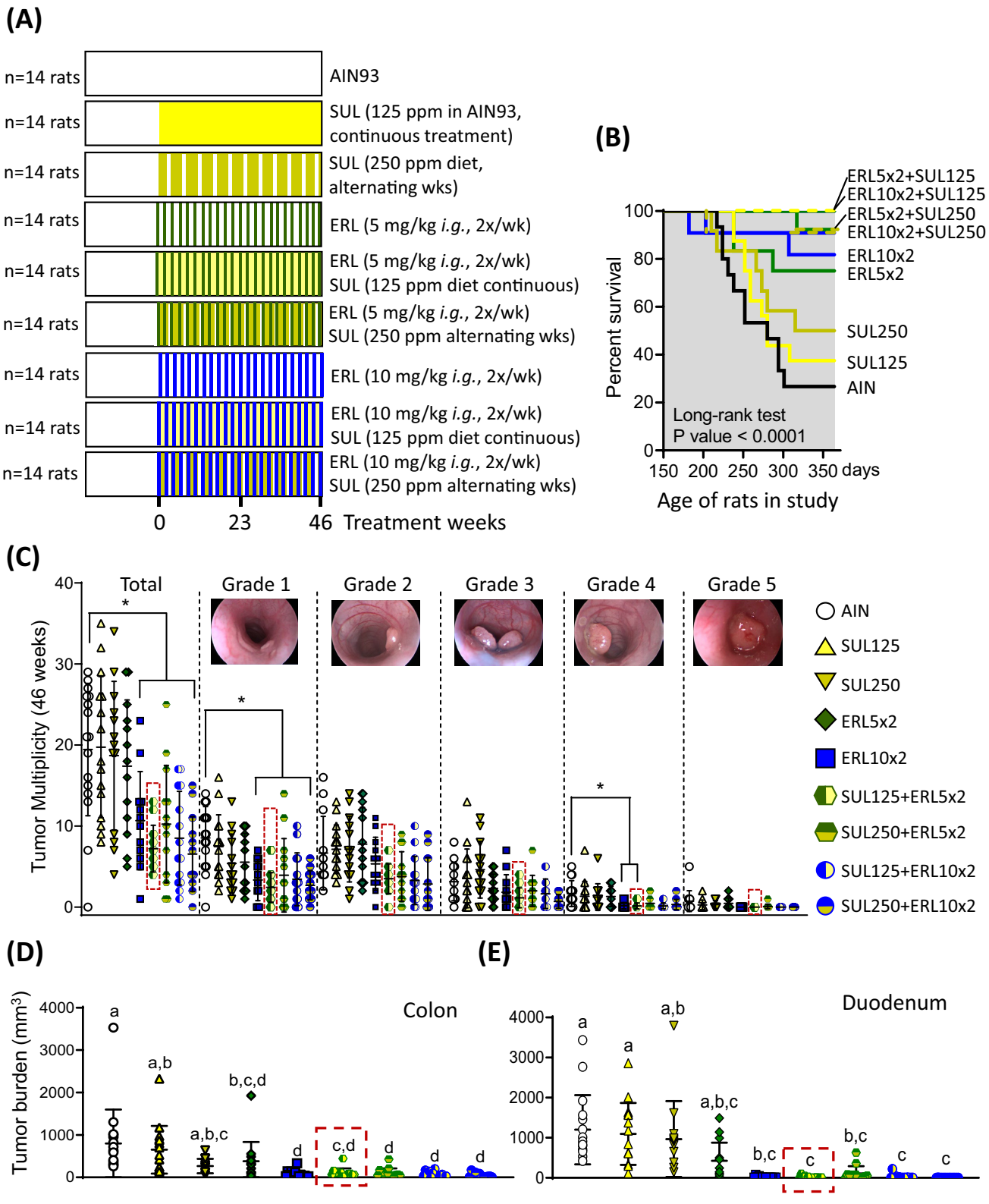

FIGURE 2 Long-term intermittent low-dose ERL ± SUL treatment suppressed Pirc colon and duodenum tumors. (A) Long-term efficacy protocol involving 46-week dosing of test agents. (B) Kaplan–Meier survival curves for rats up to 1 year of age. (C) Colonoscopic assessment of tumor burden following 29-week dosing of test agents. In the scatter plots, each observable colon tumor was represented by a datapoint; horizontal line, median. Records also were kept according to tumor size Grade 1–5, with representative images provided. *$p < 0.05$ by Student's t-test for each individual treatment group versus the corresponding AIN control. (D, E) Scatter plots of antitumor activity in the colon and duodenum of rats at 1 year, respectively, following 46-week dosing of test agents, with each animal represented by a single datapoint. Groups sharing the same superscript letter were not significantly different by one-way ANOVA.

Finetek, Torrance) to enhance tissue preservation for frozen sectioning. Frozen sections (6-μm) were cut at −20°C using a cryostat and subsequently placed on charged glass microscope slides. IMC analysis[17–20] was performed at Houston Methodist Immunomonitoring Core (Director Dr. Shu-Hsia Chen). The Fluidigm protocol was used to generate rat-specific antibodies to the following immune markers: Cd3, Cd4, Cd8, Cd11c, Cd45, Cd68, Cd206, Arg1, Foxp3, and Granzyme B (GrB). Heat-induced antigen retrieval was conducted in a temperature-controlled microwave at 95°C in Tris-Tween20 buffer at pH 9 for 20 min. After immediate cooling for 20 minutes, sections were blocked with 3% bovine serum albumin in tris-buffered saline (TBS) for 1 h. Tissue sections were incubated with antibody master mix overnight at 4°C, washed 4 times with TBS/0.1% Tween20, and stained with Cell-ID Intercalator (Fluidigm) for 5 min. Slides were washed with TBS/0.1% Tween20, air-dried, and stored at 4°C. Image collection was conducted using the Fluidigm Hyperion™ system, and following ilastik and CellProfiler segmentation, histology topography cytometry analysis toolbox (HistoCAT) and R scripts were used to quantify cell number, generate t-SNE plots, and perform neighborhood analysis.[21,22] To identify significantly enriched or depleted pairwise neighbor interactions between cell types, histoCAT functions were used to perform a permutation-test-based analysis of spatial single-cell neighborhoods.[21] Neighboring cells were defined as those within 4 pixels (4 μm). *P* values smaller than 0.05 were considered significant.

2.6 | Establishment of Pirc tumor cell lines

Screening colonoscopy[12] facilitated the selection of Pirc males with a high colon tumor burden at 9–12 months of age. For cell dissociation from colon polyps, a prior methodology[23] was used, with modification. In brief, after flushing the colon with ice-cold PBS, tumors were resected using sterile dissection tools and placed in ice-cold PBS containing 1% penicillin/streptomycin/amphotericin B (Catalog # 30-004-CI, Corning, Manassas, VA). Under sterile conditions, polyps were cut into small pieces and placed in C-tubes (catalog #130-093-237, Miltenyi Biotech, Gaithersburg, MD) containing 3 mL of IMEM (Gibco) with Tumor Dissociation Kit enzymes (catalog #130-096-730, Miltenyi Biotech, Gaithersburg, MD). After a 10-minute incubation at 37°C in a gentleMACS™ Octo Dissociator, single cells were filtered through a cell strainer into tubes containing 10 mL conditional rat tumor media, consisting of IMEM (Gibco), 20% fetal bovine serum (HyClone), antibiotics, and growth supplements, as reported.[23] Following centrifugation at 300*g* for 10 min, supernatant media was discarded, and the cell pellet was gently dissociated into 15 mL of conditional rat tumor media. Cells were incubated in a 100 mm Petri dish at 37°C and 5% CO_2. Cell attachment was detected after 10–14 days, with media replaced twice weekly. At 90% confluency, Pirc colon tumor (PCT) cells were split 1:3 for maintenance and propagation. This protocol was also applied to the establishment of Pirc duodenal tumor (PDT) cell lines.

2.7 | Cell-based assays

Rat primary PCT, PDT cells from Pirc polyps and mouse colon carcinoma MC38-OVA cells (RRID:CVCL_XJ96, provided by Dr. Arlene Sharpe, Harvard Medical School, Boston, MA) were plated at a density of 60,000 cells per well in 6-well tissue culture plates. Cells were left to attach overnight and incubated for 7 days with dimethylsulfoxide (DMSO), ERL (0.75 μM), SUL (50 μM) or ERL + SUL. In some experiments, MC38-OVA cells were treated for 7 days with scrambled or 200 pmol of pooled *Nlrc5*-targeted siRNAs (catalog #4390771, ThermoFisher Scientific, Waltham, MA), along with concurrent ERL ± SUL treatment, as reported earlier.[13] Complete media containing fresh test agents were replenished every other day. Cells were treated with 0.05% trypsin plus ethylenediaminetetraacetic acid (EDTA) and resuspended for cell viability and live cell determination. In brief, cell suspension and 0.4% trypan blue (VWR Life Science) were mixed in a 1:1 ratio and incubated for 3 min at room temperature. A volume of 10 μL was applied to a Countess™ chamber slide (Invitrogen) and cells were enumerated using an automated Countess II FL cell counter (Life Technologies). Cells were imaged via phase-contrast microscopy using a BioTek Cytation Imaging Multimode Reader at 4× or 10× magnification. After centrifugation at 10,000 rpm for 10 min and washing with phosphate-buffered saline (PBS), cell pellets were taken for IB, as above.

Furthermore, in MC38-OVA cells incubated with test agents as above, the immunoassay-based assessment of OVA-driven IL-2 secretion was performed using murine B3Z (RRID: CVCL_6277) $Cd8^+$ T cell hybridomas, which recognize OVA peptides presented on MHC class I cell surface complexes.[15] Cells were reseeded in a 24-well tissue culture plate (100,000 cells/well) and allowed to attach for 36 h. After washing twice with PBS (300 μL), B3Z hybridoma cells were added to each well (500,000 cells/well) for a final volume of 0.5 mL in complete medium and co-cultured for 24 h. MC38-OVA cells pretreated for 24 h with IFN-γ (10 ng/mL) served as a positive control. Murine IL-2 was quantified in the cell supernatant via enzyme-linked immunosorbent assay (R&D system). DMEM supplemented with 10% fetal bovine serum (FBS) and penicillin/streptomycin (10,000 U/10 mg/mL) was used as complete medium for MC38-OVA cells, whereas RPMI 1640 medium (Gibco) supplemented with L-glutamine (5 mM) was used for B3Z hybridoma cells. All experiments were performed with mycoplasma-free cells.

2.8 | FAP patient-derived organoids

Fresh colonic polyp biopsies were collected from an FAP patient at The University of Texas MD Anderson Cancer Center under an approved IRB protocol (#PA12-0327). Crypt isolation and short-term

organoid formation followed protocols previously described.[24] In brief, colonic tissues were placed immediately in DMEM/F-12 media, washed with cold PBS, and cut into 1–2 cm pieces. Tissue pieces were washed three times with PBS containing 5% fungizone, followed by incubation in PBS plus 0.5 mM EDTA at 4°C for 45 min on a rocking platform. Crypts were collected into a separate tube, and the crypt isolation procedure was repeated. Pooled crypts were pelleted by centrifugation for 5 min at 1500 rpm, resuspended in 50 mL Matrigel (catalog #CB-40230c, Corning, Corning, NY) and transferred to a 24-well plate. After incubation at 37°C, suspended crypts were cultured in complete media containing growth factors (CMGF++), as follows: Advanced DMEM/F12 Wnt/R-Spondin/Noggin conditioned medium supplemented with 1× B27 (catalog #17504-044, Invitrogen, Waltham, MA), 1× N2-supplement (catalog # 175020- 048, Invitrogen Waltham, MA), 10 mM nicotinamide (catalog #N0636, Sigma Aldrich, St. Louis, MO), 1.25 mM N-acetylcysteine (catalog #A9165, Sigma Aldrich St. Louis, MO), 50 ng/mL recombinant EGF (catalog #PMG8043, Invitrogen, Waltham, MA), Primocin (catalog #ant-pm-2, Invitrogen, Waltham, MA), 10 nM gastrin (catalog #G9145, Sigma Aldrich St. Louis, MO), 1 μM prostaglandin E2 (catalog #S3003, Selleckchem, Houston, TX), 10 μM SB202190 (catalog #S7067, Sigma Aldrich St. Louis, MO), 500 nM A83-01 (catalog #2939, Tocris, Minneapolis, MN), 0.1% 250 μg/mL amphotericin B (catalog #15290-018, Gibco, Carlsbad, CA), 10 mM HEPES (catalog #15630-080, Invitrogen, Waltham, MA), 2 mM GlutaMAX (catalog #35050-061, Invitrogen Waltham, MA), 100 U/mL penicillin/streptomycin, and 10 μM Y-27632. Organoids were cultured over an approximate 30-day period at 37°C, with fresh media changes every 2–3 days, and passaged every 1–2 weeks until a full 24-well plate was achieved.

Organoids were treated in CMFG++ growth media for 7 days with 25 nM ERL, 25 μM SUL, 25 nM ERL + 25 μM SUL, or DMSO. Every other day, media was aspirated and replenished with fresh media containing ERL ± SUL. On the seventh day, organoids were imaged via bright-field microscopy at 4× magnification and harvested using 300 μL of Cell Recovery Solution (catalog #354253, Corning, NY). The cell suspension was placed on ice for 45 min and centrifuged at 5,000 rpm for 5 min. RNA was isolated from pooled organoid samples for RT-qPCR analysis, following the procedures mentioned above.

2.9 | Statistical analyses

Unless indicated otherwise, data were presented as mean ± SE from three or more biological and technical replicates. Paired group comparisons were made for treatment versus control using Student's *t*-test, whereas group comparisons were made via ANOVA with Tukey multiple comparison test in GraphPad Prism 9.5.1. In the figures, datasets sharing the same superscript letter did not differ significantly by ANOVA,[14–16] whereas an asterisk designates significance at the $^{*}p < 0.05$ level for paired *t*-tests. Other results were presented as scatter plots, with each data point representing an individual tumor.

3 | RESULTS

3.1 | Intermittent low-dose SUL + ERL treatment suppressed colon and duodenal polyps

We reported on antitumor outcomes in the Pirc model using the standard of care equivalent dose of SUL plus oral administration of ERL once a week, rather than daily,[7] which translated successfully to FAP patients.[8] To explore the lower limit of combinatorial ERL + SUL efficacy, additional intermittent dosing protocols were devised (Figure 1A). Paralleling the prior methodology,[7] Pirc males ($n = 10$ rats/group) at 6 weeks of age were fed an AIN3 basal diet or an AIN diet containing 250 ppm SUL, alone or in combination with ERL at 10 mg/kg BW by weekly oral gavage administration (ERL10). Other groups received ERL twice a week at 5 or 10 mg/kg BW (ERL5 × 2 and ERL10 × 2). Colonoscopy revealed a time-dependent increase in tumor number for AIN controls and near-complete suppression by ERL5 × 2 + SUL, with intermediate efficacy for other groups (Figure 1B).

Dose-dependent inhibition of total tumor burden was observed for ERL alone and in combination with SUL after 16 weeks of drug treatment (Figure 1C,D). Antitumor efficacy was especially marked in the duodenum (Figure 1D) compared to the colon (Figure 1C) and for combination groups ERL5 × 2 + SUL, ERL10 + SUL, and ERL10 × 2 + SUL. Target modulation was also confirmed in tumors through pErk levels, as exemplified by comparisons of ERL10, SUL250, and ERL10 + SUL250 compared with AIN controls in the colon (Figure 1E) and duodenum tumors (Figure 1F). However, despite the greater inhibition of pErk in colon (Figure 1G) versus duodenal tumors (Figure 1H), this did not correlate with the stronger antitumor efficacies seen in the duodenum (Figure 1D) versus the colon (Figure 1C). Efficacy was also maintained with half the standard SUL dose, whether administered continuously at 125 ppm or on a bi-weekly schedule of 250 ppm (Figure S1).

In a subsequent long-term investigation lasting 1 year (Figure 2A), Pirc males ($n = 14$ rats/group) starting at 6 weeks of age were given test agents for 46 weeks, as follows: (i) SUL continuously in the diet at 125 ppm (SUL125); (ii) SUL250 on alternating weeks; (iii) bi-weekly ERL at 5 or 10 mg/kg (ERL5 × 2 or ERL10 × 2); and (iv) the corresponding ERL + SUL combinations. Individual rats that became moribund due to a high tumor burden were euthanized early. The corresponding Kaplan-Meier curves reflected a lower percent survival in AIN and SUL alone groups compared to 100% survival after ERL5 × 2 + SUL125 and ERL10 × 2 + SUL125 combinations, with intermediate survival for other groups (Figure 2B). A record was kept of each lesion observed during monthly colonoscopy, and a final tally was made of the corresponding tumor multiplicity and tumor size, ranging from Grade 1 to Grade 5 (Figure 2C). Significant inhibition occurred in multiple treatment groups and across all polyp sizes, with Grade 1 lesions exhibiting particularly marked tumor suppression. The lowest combinatorial treatment that yielded statistically significant tumor inhibition was SUL125 + ERL5 × 2 (dashed boxes, Figure 2C).

Post-necropsy analysis confirmed these findings in both colon (Figure 2D) and duodenum (Figure 2E), the latter not being amenable

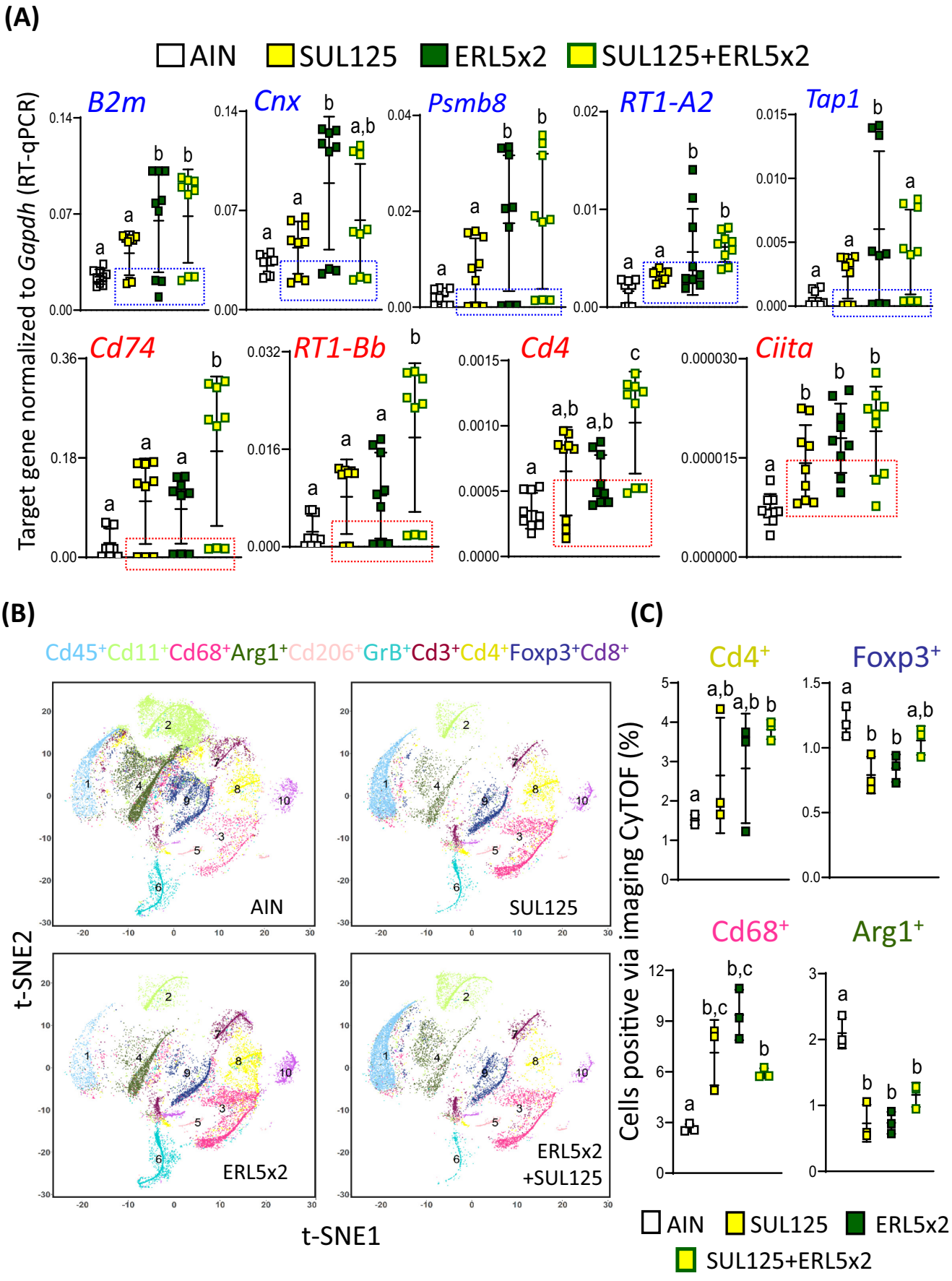

FIGURE 3 Legend on next page.

to colonoscopy, with the lowest effective combinatorial treatment regimen being SUL125 + ERL5 × 2 (dashed boxes, Figure 2D,E). Subsequently, the SUL125 + ERL5 × 2 low-dose efficacy 'window' was advanced into immune-related analyses.

3.2 | Intermittent SUL ± ERL increased MHC expression and altered the immune cell niche

Based on transcriptomic data from FAP patients after a 6-month intervention with ERL + SUL, which prioritized interferon-γ (IFN-γ) signaling among other pathways,[10] we next examined immune endpoints in Pirc colon tumors at 1 year. RT-qPCR analyses revealed significant induction of murine MHC class I genes (*B2m*, *Cnx*, *Psmb8*, *RT1-A2*, and *Tap1*) and class II genes (*Cd74*, *RT1-Bb*, *Cd4*, and *Ciita*) in treatments with SUL125, ERL5 × 2, and their combination compared with the AIN group (Figure 3A). Interestingly, a subpopulation of tumors remained resistant to MHC upregulation following ERL ± SUL dosing (dashed boxes, Figure 3A).

Corroboration of the gene expression data at the protein level was conducted via IB, IHC, or imaging mass cytometry (IMC) (Figures 3B,C and S2A–D). Following treatment with SUL125, ERL5 × 2, or the combination, IB revealed high Cd74 protein expression in duodenal tumors, and both the colon and duodenal tumors exhibited markedly increased B2m levels (Figure S2A, dashed boxes). Elevated B2m protein expression was also observed via IHC analysis in colon tissues and tumors from Pirc rats treated with ERL±SUL (Figure S2D).

Pirc tumors collected at 1 year were also examined via IMC, and the data were visualized using t-SNE plots (Figure 3B). Quantitative analysis confirmed that both single and combined test agents caused statistically significant increases in tumor-associated $Cd4^+$ and $Cd68^+$ cells while decreasing $Foxp3^+$ and $Arg1^+$ cells compared to AIN (Figures 3C and S2B). Interestingly, no drug-related changes were observed for tumor-infiltrating $Cd8^+$ cells compared with AIN controls (Figure S2C).

Given the observed decrease in $Arg1^+$ cells by ERL ± SUL (Figure 3C), we examined another M2 macrophage marker in Pirc tumors at 1 year, namely, Cd163.[25] RT-qPCR revealed that ERL5 × 2 ± SUL125 lowered *Cd163* expression significantly, with some tumors also being responsive in the SUL125 group compared to AIN controls (dashed box, Figure 4A). IB analyses corroborated these findings, showing reduced Cd163 protein expression in ERL5 × 2, SUL125, SUL250, and their combinations, relative to AIN controls in the colon (Figure 4B) and duodenum tumors (Figure 4C). Quantification of densitometry data confirmed statistically significant inhibition of Cd163 expression for ERL5 × 2, SUL250, and their combination in colon tumors (Figure 4D), and for ERL5 × 2, SUL250 + ERL5 × 2, and SUL125 + ERL5 × 2 groups in duodenal polyps (Figure 4E).

3.3 | MHC factors downregulated in large tumors were increased by ERL ± SUL treatment

Polyps in size grades 1–5 (Figure 2C) exhibited a progressive increase in MHC class I gene expression for *B2m*, *Psmb8*, *Cnx*, *Tap2*, and for MHC class II genes *Cd74*, *RT1-Bb*. However, this upregulation was markedly reversed in lesions larger than Grade 5, that is, >150 mm^3 (Figure 5A, dashed boxes). Rat PCT and mouse MC38-OVA cells incubated ex vivo for 7 days with 0.75 μM ERL, 50 μM SUL, or the combination agents exhibited no significant changes in cell viability or count (Figure 5B–E), and IB revealed no increase in cleaved PARP, consistent with a lack of apoptosis induction (Figure 5F,G, arrows). However, MHC class I-related proteins Nlrc5, B2m, Psmb8, Psmb9, and Tap1 were induced by ERL ± SUL treatment compared to vehicle controls, with the results for ERL in PCT cells being particularly striking (Figure 5F, dashed box). One notable observation was that PCT cells exhibited high basal MHC-I (rat RT-1A) levels and no apparent increase by the test agents (Figure 5F), whereas MC38-OVA cells had low constitutive MHC-I (mouse H-2d) expression, which was induced by SUL ± ERL after 7 days (Figure 5G). Using a reported co-culture system,[15] Il-2 production from B3Z cells corroborated that cell surface occupancy of functional MHC-I complexes was significantly increased on MC38-OVA colon cancer cells, in the relative order: DMSO < ERL + SUL < SUL = ERL < IFN-γ (Figure 5H). IB in MC38-OVA cells following siRNA-mediated knockdown of Nlrc5 revealed that Nlrc5 interference attenuated the inducibility of B2m and other components of the MHC class I pathway in response to ERL ± SUL treatment (Figure 5I,J).

3.4 | B2M was induced in FAP patient-derived organoids treated with ERL ± SUL ex vivo

Finally, based on pilot studies into the optimal dose and timing of exposure, FAP patient-derived colon organoids were incubated with 25 nM ERL (ERL25), 25 μM SUL (SUL25), or the combination for 7 days. No marked phenotypic changes or signs of overt toxicity occurred under the experimental conditions employed (Figure 6A). However, significant upregulation of the MHC class I prototypic gene *B2M* was observed by ERL ± SUL treatment (Figure 6B), and a working model was proposed to summarize treatment effects on the MHC-I pathway, integrating insights from both patient-derived organoids and PCT cells (Figure 6C).

FIGURE 3 Long-term intermittent low-dose SUL ± ERL treatment increased MHC gene expression in a sub-population of Pirc tumors at 1 year and altered the immune cell niche. (A) Scatter plots of MHC class I and II gene expression assessed by RT-qPCR and normalized to *Gapdh*; horizontal line, median. Data are representative of three or more independent experiments, with $n = 9$ colon tumors per treatment group. (B) IMC data were visualized as t-SNE plots for selected markers of the immune cell niche in Pirc colon tumors at 1 year. (C) IMC data quantified ($n = 3$ tumors per group) revealed significant drug-induced changes in the percentage of $Cd4^+$, $Cd68^+$, $Foxp3^+$, and $Arg1^+$ cells. In panels (A) and (C), groups with the same superscript letter were not significantly different by one-way ANOVA.

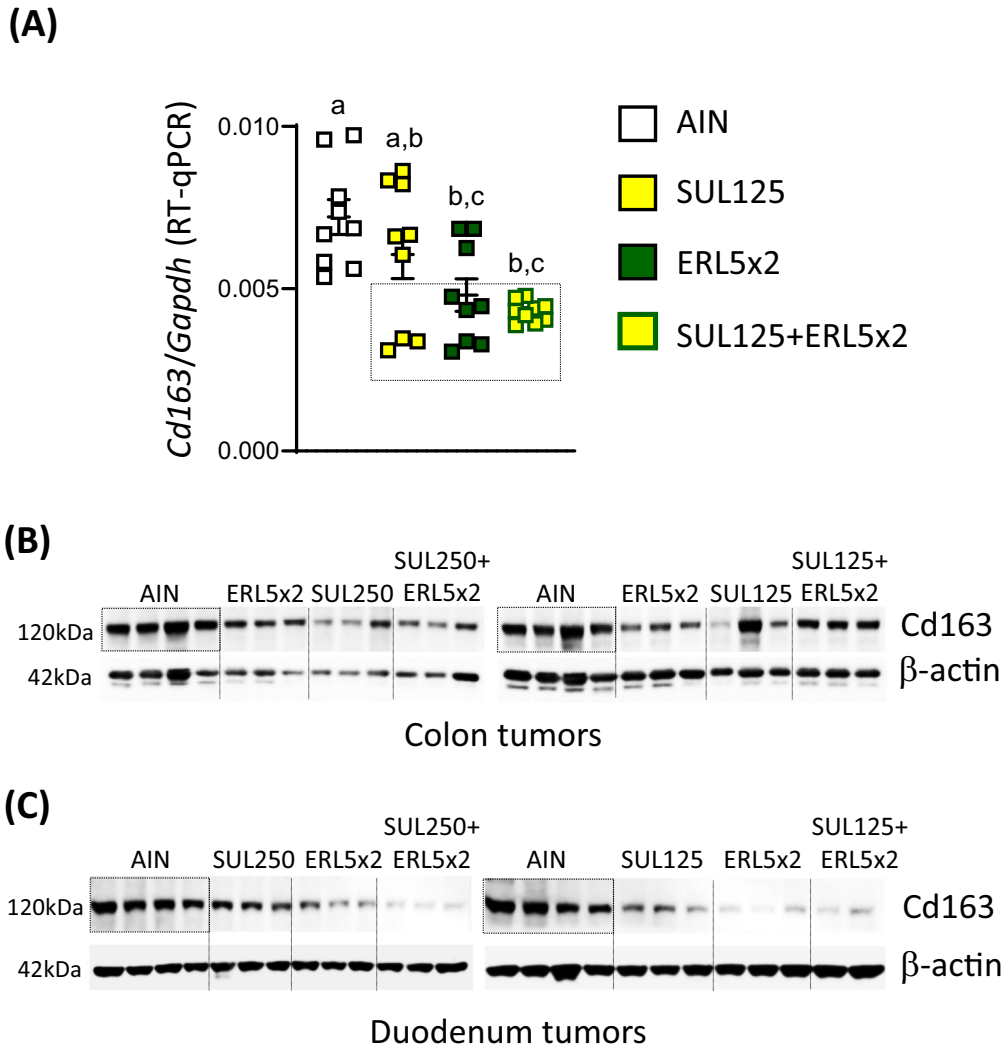

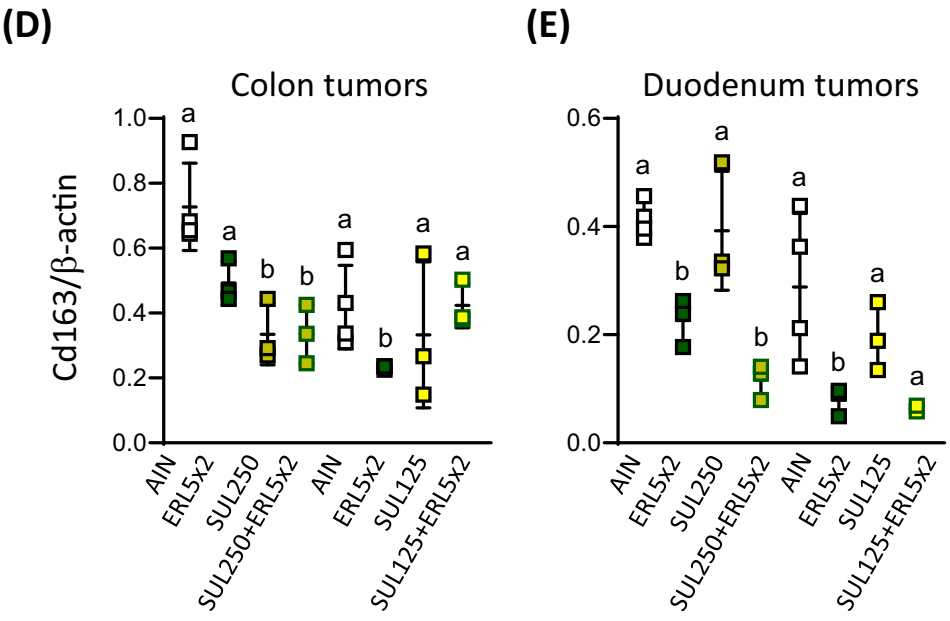

FIGURE 4 Long-term intermittent low-dose SUL ± ERL treatment reduced Cd163 expression in Pirc colon and duodenum tumors. (A) Scatter plot of *Cd163* gene expression in Pirc colon tumors at 1 year assessed by RT-qPCR and normalized to *Gapdh*; horizontal line, median. Data are representative of three or more independent experiments ($n = 9$ tumors per group). Immunoblots of Cd163 expression in (B) Pirc colon and (C) Pirc duodenum tumors at 1 year, with β-actin as loading control. Each lane represents a single tumor, and data are representative of three or more independent experiments. (D, E) Quantification of data in panels (B, C) respectively, by densitometry. In the scatter plots, groups sharing the same superscript letter were not significantly different by one-way ANOVA.

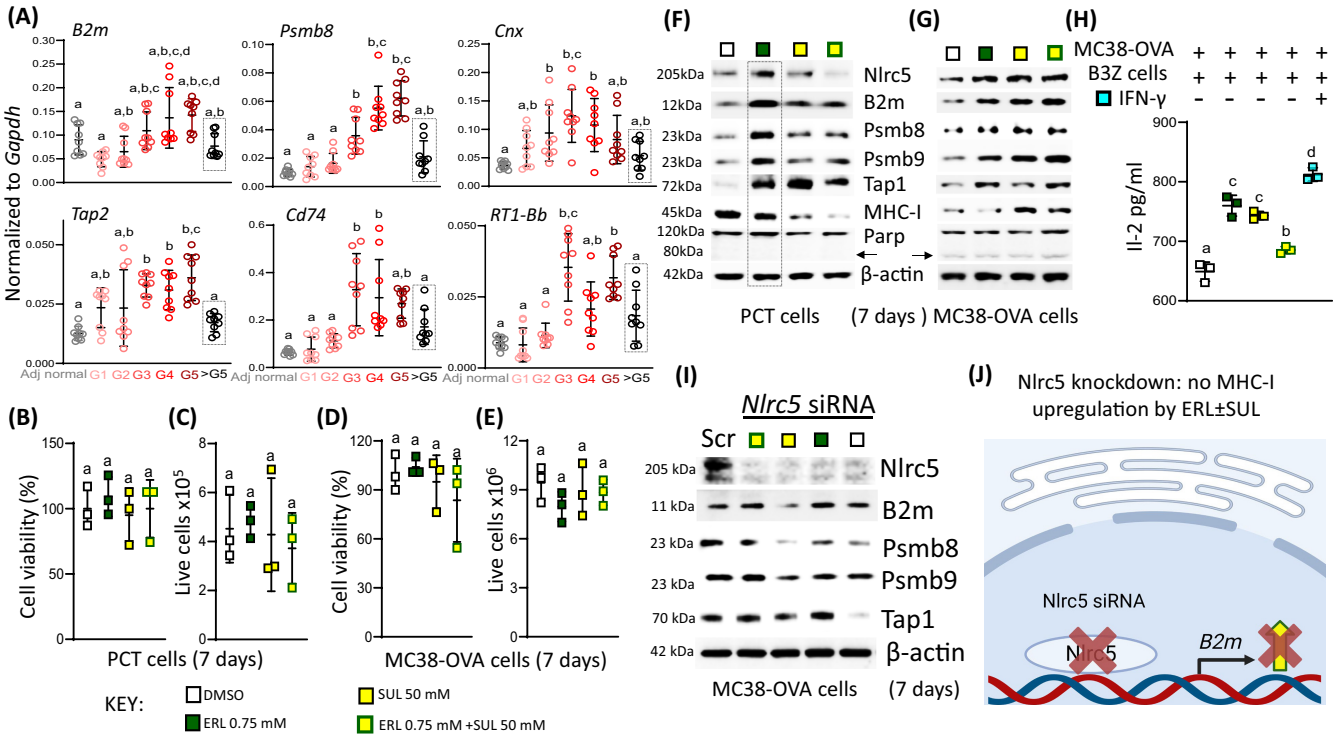

FIGURE 5 Pirc tumors exhibit decreased MHC gene expression in large polyps, with reversibility demonstrated by ex vivo SUL ± ERL treatment. (A) Scatter plots of MHC class I and II gene expression assessed by RT-qPCR and normalized to *Gapdh*; median, horizontal line. Data are representative of three or more independent experiments ($n = 9$ colon tumors per group). G1–G5 signifies polyp size (see Figure 2C), with occluding lesions being larger than 150 mm^3 (>G5); Adj, adjacent. (B, C) Pirc colon tumor (PCT) and (D, E) mouse MC38-OVA colon carcinoma cells incubated for 7 days with 0.75 mM ERL, 50 mM SUL, or ERL + SUL exhibited no significant changes in viability or live cell number compared to vehicle controls. No phenotypic alterations were observed after a 7-day treatment with test agents (Figure S8). Immunoblots of (F), PCT and (G), MC38 cells after 7-day treatment with SUL ± ERL, as in panels (B–E). MHC-related proteins were normalized to β-actin. Poly(ADP-ribose) polymerase (PARP) served as an apoptosis marker. In PCT and MC38-OVA cells, MHC-I refers to rat RT-1A and mouse H2-d proteins, respectively. (H) Immunoassay-based assessment of interleukin-2 (Il-2) secretion in a co-culture assay, as reported,[15] with IFN-γ as the positive control. (I) Immunoblots of MC38-OVA cells transfected with Nlrc5 siRNA (200 pmol) and treated concomitantly with ERL (0.75 μM) ± SUL (50 μM) for 7 days. β-actin served as loading control. Scrambled siRNA served as negative control. (J) Working model for the non-inducibility of MHC-I pathway members following Nlrc5 KD (image created using software from BioRender.com, accessed on May 30, 2024). In panels A, B and D, groups sharing the same superscript letter were not significantly different by one-way ANOVA.

4 | DISCUSSION

In this investigation, we report that intermittent, low-dose treatment with SUL±ERL significantly inhibited tumor growth by upregulating MHC class I and II expression and remodeling the immune cell niche in an Apc-mutant model of FAP. The drug combination strategy not only unveiled new insights into immune modulation but also highlighted the synergy between SUL+ERL treatment and the crucial role of dose optimization for enhanced therapeutic benefit while minimizing toxicity. In addition to the knowledge gained in these matters, our findings also underscored the necessity for further research into the specific contributions of the associated MHC pathways.

Our initial working hypothesis was that epigenetic silencing mechanisms might cause a progressive loss of MHC class I and II antigen presentation, as a means of keeping early adenomas immunologically quiescent and contributing to immune evasion. While this hypothesis was partially supported by the observed downregulation of *B2m*, *Psmb8*, *Cnx*, *Tap2*, *Cd74*, and *RT-1Bb* in the largest tumors, the data revealed a more nuanced scenario. Notably, smaller adenomas demonstrated increased MHC expression, which sharply declined in tumors larger than Grade 5. This finding provides a critical juncture for immune interception in the Pirc model, with implications for both genetic and sporadic cancer etiology in the gut. It appears that early adenomas sought to elevate MHC expression to engage immune surveillance, yet failed to maintain this situation, leading to ineffective T-cell priming and immune evasion. Such observations might relate to the fact that larger lesions likely have high-grade dysplasia accompanied by the local invasion of neoplastic cells into the stalk, classifying the tumors as adenocarcinomas.[6]

As proof of principle, tumors from patients with microsatellite stable colorectal cancer—which would include at-risk FAP kindreds—had clonal predicted neoantigens, but their low expression interfered with productive T-cell priming, leading to T cell dysfunction.[26] Therapeutic rescue of priming rendered T cells able to control tumors with low neoantigen expression, underscoring a key role for neoantigen expression levels in immune evasion.[26] The observation that intermittent

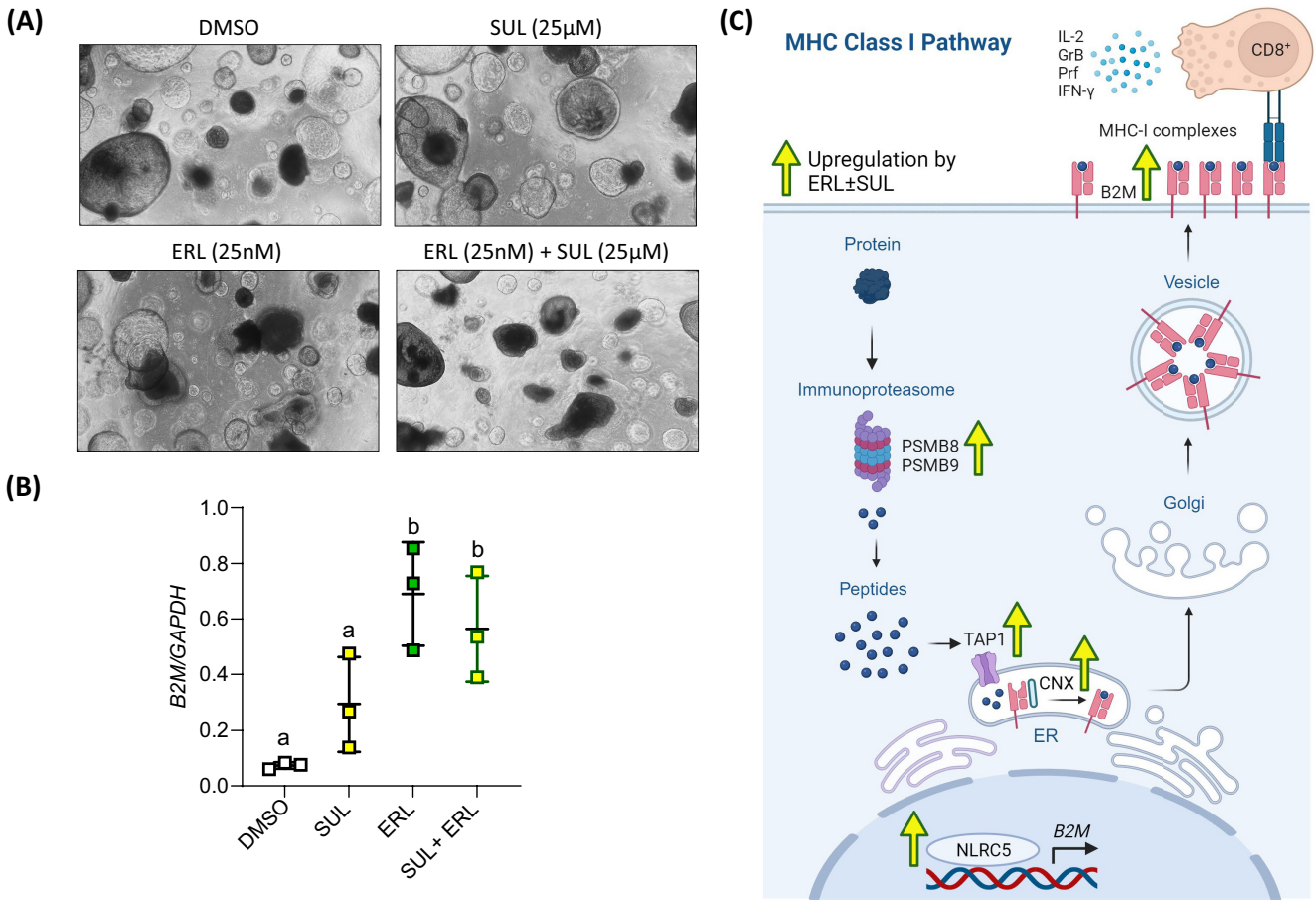

FIGURE 6 The prototypical MHC class I-dependent gene *B2M* is upregulated by ERL ± SUL treatment in FAP patient-derived colon organoids. (A) Representative bright-field microscopy images of FAP patient-derived colon organoids at 4× magnification after 7-day treatment with SUL, ERL, or ERL + SUL at the concentrations indicated. No marked phenotypic changes were observed or signs of overt toxicity. (B) Upregulation of *B2M* expression after treatment with test agents, as in panel (A), assessed by RT-qPCR and normalized to *GAPDH*; horizontal line, median. Groups sharing the same superscript letter were not significantly different by one-way ANOVA. (C) Working model for MHC class I pathway and its upregulation by ERL ± SUL in Pirc tumors and FAP patient-derived organoids (image created using software from BioRender.com, accessed on January 26, 2024). IFN-γ, interferon-γ; IL-2, interleukin-2; GrB, granzyme B; Prf, perforin.

low-dose ERL±SUL treatment circumvented MHC downregulation in Pirc tumors, while a subpopulation of polyps remained resistant, warrants further investigation. Previous studies demonstrated that MHC downregulation can occur in gastrointestinal malignancies due to the deposition of suppressive epigenetic marks that silence gene expression, such as DNA methylation and histone modifications.[27] Consequently, such aberrant epigenetic signatures might contribute to the observed lack of MHC induction in a subset of resistant polyps following ERL ± SUL treatment (Figure 3A, dashed boxes).

Interestingly, Nlrc5 interference markedly attenuated the inducibility of B2m and other components of the MHC class I pathway in response to ERL ± SUL treatment (Figure 5I,J). Thus, the ability of the test agents to induce MHC class I-associated factors was most likely dependent on the presence of Nlrc5, a "master" transcriptional regulator of MHC-I gene expression.[28] This observation suggests that epigenetic downregulation of Nlrc5 might have a key role in circumventing MHC-I induction in resistant colon polyps after ERL ± SUL administration. However, epigenetic silencing marks deposited in promoter or enhancer regions of other MHC-related genes cannot be excluded and warrant further investigation, as exemplified for inhibitors of the PRC2 complex that restore MHC expression in lung and hematologic malignancies.[29] Epigenome profiling studies are now in progress examining multiple MHC-I and MHC-II epigenetic regulatory mechanisms in Pirc tumors and FAP patient-derived organoids following ERL ± SUL treatment. The goal is to design new combinatorial strategies that incorporate ERL or SUL alongside novel inhibitors of epigenetic readers, writers, or erasers. Such combinatorial approaches might overcome the resistance observed in colon and duodenal polyps, in terms of MHC upregulation, leading to enhanced antitumor immune responses and improved outcomes for FAP patients. The significant induction of *B2M* expression in FAP patient-derived colon organoids incubated with ERL ± SUL provided proof-of-principle for an immune-based approach to precision medicine, based on the current working model (Figure 6C). For other resistant polyps, anti-Egfr monoclonal antibody might be considered, targeting Egr1 turnover and reduced immunosuppressive chemokines to repel

Tregs and M2 macrophages while recruiting $Cd8^+$ T cells into the tumor microenvironment.[30]

Our results highlighted the critical role of $Cd4^+$ T cells, which not only assist in priming and activating Cd8+ T cells, but can also exert direct antitumor effects, thereby contributing to the efficacy of intermittent low-dose ERL + SUL treatment. The need also exists for additional investigation into activated Cd8+ T cells, particularly through markers such as PD-1, CTLA-4, Granzyme B, OX40, and LAG-3.[26] Despite observing no apparent changes in $Cd8^+$ T cell recruitment into Pirc colon polyps after drug treatment, IMC data revealed that intermittent low-dose ERL + SUL administration increased tumor-associated $Cd4^+$ and $Cd68^+$ cells while reducing $Foxp3^+$ and $Arg1^+$ cells. These data suggested a shift towards a permissive "helper" immune environment, including diminished immunosuppressive Tregs and altered M1/M2 macrophage polarization. This shift is of interest given the ongoing debate over the various markers of tumor-associated macrophages and their prognostic value in colorectal cancer patients.[25,31–38] In the present investigation, an increase in $Cd68^+$ cells and decreased $Arg1^+$ cells after drug treatment implicated a shift away from tumor-promotional M2 macrophages towards tumor-suppressive M1 macrophages.[11] By spatial immune profiling, a low $CD68^+/CD163^+$ cell ratio in the tumor core was associated with improved disease-free survival in colorectal cancer patients.[25] However, the current investigation detected a higher $Cd68^+/Cd163^+$ ratio, typically associated with poor prognosis, which contrasted with the observed antitumor efficacy, suggesting a more complex relationship between macrophage subtype and tumor stage.[39–43]

Beyond the immune endpoints discussed here, intermittent low-dose ERL ± SUL treatment in the Pirc model inhibited other tumor-associated biomarkers at 1 year, including pErk, Mmp7, β-catenin, Cox2, and Il1-β (Figure S3). These findings align with transcriptomic data from FAP patients given ERL+SUL that prioritized EGFR, PGE2/COX, and WNT signaling along with IFN-γ regulation.[10] Interestingly, clinical trials with agents such as Naproxen provided evidence for immune activation in colorectal mucosa, reinforcing the importance of considering both immune and non-immune modulatory mechanisms of NSAIDs in patients.[44–46] Interestingly, in a preclinical model of colitis, myeloid-specific but not epithelial cell-specific deletion of Egfr in the intestine decreased tumor multiplicity, protected against high-grade dysplasia, and reduced both M1 and M2 macrophages.[47] Independent of the immune cell component, we observed that ERL ± SUL treatment caused marked changes in FAP patient-derived colon organoids, Pirc colon tumor lines, and murine colon adenocarcinoma cells in support of the working model (Figure 6C). Future research might incorporate co-culture of $CD4^+$ and/or $CD8^+$ T cells with FAP patient-derived organoids while accounting for HLA compatibility. At the doses employed for ERL+SUL and for other low-dose test agent combinations that might be translated to FAP kindreds, it will be important to consider the immune microenvironment in the adenoma-carcinoma sequence.[11] Spatial immune-profiling[25] provides an attractive avenue for precision immune-interception, in which deleterious alterations in the immune cell niche might be identified and corrected on a case-by-case basis for improved patient-specific targeted intervention.

In agreement with the predictions from our prior studies in the Pirc model,[7] switching from daily to weekly drug treatment maintained antitumor efficacy in FAP patients.[8] However, adverse events still occurred in nearly three-quarters of the participants who took weekly ERL for 6 months.[8] Adverse events might have been alleviated using one-quarter of the standard of care for ERL plus one-half for SUL, while retaining significant antitumor efficacy in the colon and duodenum according to the current investigation. As expected from our prior studies in the Pirc model,[7] the intermittent low-dose ERL ± SUL treatment protocols used here had no adverse effects on body weight gain, organ weight, gastric ulcer index, or blood biochemistry parameters (Figures S4–S7, Table S1). There was no drug toxicity, and any mortality/morbidity was due to disease pathogenesis in the Apc-mutant genetic background, as reported.[6] Future work should consider whether drug doses that lacked overt toxicity or apoptosis-inducing activity in intestinal mucosal cells affected naïve T-cells or other components of the "helper" immune cell niche to impact T-cell priming and potential therapy response.[26] These aspects are currently being pursued in the Pirc model. In cell-based assays, ERL ± SUL concentrations were chosen carefully from prior reports[48–51] and pilot experiments (Figure S8) to avoid marked phenotypic changes after 7 days of treatment.

Finally, key observations in rat colon tumor cells were recapitulated in Pirc duodenum tumor cells. For example, PDT cells treated with 0.75 μM ERL for 7 days exhibited marked induction of MHC class I-related proteins, such as B2m and Nlrc5, without adverse effects on viability, live cell number, or overall phenotype (Figure S9). Thus, the immunomodulatory mechanisms of ERL might be extrapolated to duodenal polyps, including in FAP patients who have undergone a colectomy, although further dose optimization will be required. Our findings highlight the possibility of combining ERL with immunotherapies or next-generation epigenetic agents.[52] Lessons learned from at-risk kindreds might translate to precancer stages in sporadic disease, beyond FAP, incorporating predictive markers from single-cell and liquid biopsy approaches.[53,54] Thus, the potential exists for more widespread applicability of the underlying immune interception concepts, with a view to advancing prevention and treatment modalities for various other human malignancies.

AUTHOR CONTRIBUTIONS

Chakrapani Tripathi: Methodology; investigation; writing – original draft; formal analysis; data curation. **Jorge E. Tovar Perez:** Methodology; investigation; formal analysis; data curation. **Sabeeta Kapoor:** Methodology; investigation; formal analysis; data curation. **Ahmed Muhsin:** Methodology. **Wan Mohaiza Dashwood:** Methodology; data curation; investigation. **Yunus Demirhan:** Methodology. **Melek Demirhan:** Methodology. **Alessandro Shapiro:** Methodology. **Altaf Mohammed:** Conceptualization; funding acquisition; supervision. **Shizuko Sei:** Conceptualization; funding acquisition; supervision. **Jacklyn**

Thompson: Methodology. **Mahira Zaheer:** Methodology. **Krishna M. Sinha:** Methodology; supervision. **Powel H. Brown:** Supervision. **Michelle I. Savage:** Project administration. **Eduardo Vilar:** Conceptualization; supervision; funding acquisition; resources. **Praveen Rajendran:** Conceptualization; supervision; funding acquisition; investigation; writing – review and editing; formal analysis. **Roderick H. Dashwood:** Conceptualization; investigation; funding acquisition; writing – review and editing; formal analysis; supervision; resources.

ACKNOWLEDGMENTS

Dr. Ahmet Ulusan and Trace Gustafson assisted with oral gavage and necropsy, whereas Dr. Pankaj Singh contributed corroborative IMC analysis for data provided by the Houston Methodist Immunomonitoring Core (Director Dr. Shu-Hsia Chen). Experiments involving antibodies were conducted in consultation with the Antibody and Biopharmaceuticals Core (ABC). Murine colon adenocarcinoma MC38 and MC38-OVA cells were kindly provided by Dr. Arlene Sharp (Harvard University, Cambridge, MA). Pirc colonoscopy images were captured by Dr. Furkan Ertem (current affiliation University of Pittsburgh Medical Center and Spartan Regional Healthcare, Spartanburg, SC). This research was supported by Task Orders 75N91019D00021 and 75N91019F00130 from the NCI PREVENT Program, under Contract No: 75N91024D00004 "PREVENT Cancer Preclinical Drug Development Program: Preclinical Efficacy and Intermediate Endpoint Biomarkers." R. Dashwood was also supported by grants CA122959 and CA257559 from the NCI and by the John S. Dunn Foundation. Funding was also provided by grant P30 CA016672 (US NIH/NCI) to the University of Texas MD Anderson Cancer Center Core Support Grant and by a gift from the Feinberg Family to E. Vilar.

FUNDING INFORMATION

Funded by Task Orders 75N91019D00021 and 75N91019F00130 from the NCI PREVENT Program, under Contract No: 75N91024D00004 "PREVENT Cancer Preclinical Drug Development Program: Preclinical Efficacy and Intermediate Endpoint Biomarkers." R.H. Dashwood was also supported by NCI grants CA122959 and CA257559, and by the John S. Dunn Foundation. Funding was also provided by grant P30 CA016672 (US NIH/NCI) to the University of Texas MD Anderson Cancer Center Core Support Grant and a gift from the Feinberg Family to E. Vilar.

CONFLICT OF INTEREST STATEMENT

E. Vilar has consulting/advisory roles with Janssen Research, Recursion Pharma, Guardant Health (Sept 2022), Rising Tide Foundation (May 2023), Nouscom, Abbvie, and research support from Janssen Research. P.H. Brown is a stockholder in GeneTex (less than 1%), which is unrelated to this work. The other authors declare no potential conflicts of interest.

DATA AVAILABILITY STATEMENT

The data that support the findings of this study are available from the corresponding author upon reasonable request.

ETHICS STATEMENT

Ethical approval for animal studies was provided by Texas A&M's IACUC (2023-0087-H) and human samples were approved by The University of Texas MD Anderson Cancer Center's IRB (PA-12-0327). This study utilized de-identified clinical samples and was therefore considered IRB exempt, with no patient consent deemed necessary.

ORCID

Chakrapani Tripathi https://orcid.org/0000-0002-0370-5829
Praveen Rajendran https://orcid.org/0000-0002-6221-7366
Roderick H. Dashwood https://orcid.org/0000-0003-0351-4034

TWITTER

Praveen Rajendran *praveendran*

REFERENCES

1. Penny HL, Prestwood TR, Bhattacharya N, et al. Restoring retinoic acid attenuates intestinal inflammation and tumorigenesis in *Apc*$^{Min/+}$ mice. *Cancer Immunol Res*. 2016;4:917-926.
2. Lynch P. Chemoprevention of familial adenomatous polyposis. *Fam Cancer*. 2016;15:467-475.
3. Kemp Bohan PM, Mankaney G, Vreeland TJ, et al. Chemoprevention in familial adenomatous polyposis: past, present and future. *Fam Cancer*. 2021;20:23-33.
4. Samadder NJ, Neklason DW, Boucher KM, et al. Effect of sulindac and erlotinib vs placebo on duodenal neoplasia in familial adenomatous polyposis: a randomized clinical trial. *Jama*. 2016;315(12):1266-1275. doi:10.1001/jama.2016.2522
5. Samadder NJ, Kuwada SK, Boucher KM, et al. Association of sulindac and erlotinib vs placebo with colorectal neoplasia in familial adenomatous polyposis: secondary analysis of a randomized clinical trial. *JAMA Oncol*. 2018;4:671-677.
6. Amos-Landgraf JM, Kwong LN, Kendziorski CM, et al. A target-selected *Apc*-mutant rat kindred enhances the modeling of familial human colon cancer. *Proc Natl Acad Sci USA*. 2007;104:4036-4041.
7. Ulusan AM, Rajendran P, Dashwood WM, et al. Optimization of erlotinib plus sulindac dosing regimens for intestinal cancer prevention in an Apc-mutant model of familial adenomatous polyposis (FAP). *Cancer Prev Res (Phila)*. 2021;14(3):325-336. doi:10.1158/1940-6207.CAPR-20-0262
8. Samadder NJ, Foster N, McMurray RP, et al. Phase II trial of weekly erlotinib dosing to reduce duodenal polyp burden associated with familial adenomatous polyposis. *Gut*. 2023;72(2):256-263. doi:10.1136/gutjnl-2021-326532
9. Lubet RA, Szabo E, Iwata KK, et al. Effect of intermittent dosing regimens of erlotinib on methylnitrosourea-induced mammary carcinogenesis. *Cancer Prev Res (Phila)*. 2013;6:448-454.
10. Delker DA, Wood AC, Snow AK, et al. Chemoprevention with cyclooxygenase and epidermal growth factor receptor inhibitors in familial adenomatous polyposis patients: mRNA signatures of duodenal neoplasia. *Cancer Prev Res (Phila)*. 2018;11:4-15.
11. Yang J, Wen Z, Li W, et al. Immune microenvironment: new insight for familial adenomatous polyposis. *Front Oncol*. 2021;11:570241.
12. Ertem F, Dashwood WM, Rajendran P, Raju G, Rashid A, Dashwood R. Development of a murine colonoscopic polypectomy model with videos. *Gastrointest Endosc*. 2016;83:1272-1276.
13. Rajendran P, Johnson G, Li L, et al. Acetylation of CCAR2 establishes a BET/BRD9 acetyl switch in response to combined deacetylase and bromodomain inhibition. *Cancer Res*. 2019;79:918-927.
14. Wang R, Dashwood WM, Nian H, et al. NADPH oxidase overexpression in human colon cancers and rat colon tumors induced by

2-amino-1-methyl-6-phenylimidazo[4,5-*b*]pyridine (PhIP). *Int J Cancer*. 2011;128:2581-2590.
15. Chen YS, Li J, Neja S, et al. Metabolomics of acute vs. chronic spinach intake in an Apc-mutant genetic background: linoleate and butanoate metabolites targeting HDAC activity and IFN-γ signaling. *Cells*. 2022; 11:573.
16. Kang Y, Nian H, Rajendran P, et al. HDAC8 and STAT3 repress BMF gene activity in colon cancer cells. *Cell Death Dis*. 2014;5:e1476.
17. Giesen C, Wang HAO, Schapiro D, et al. Highly multiplexed imaging of tumor tissues with subcellular resolution by mass cytometry. *Nat Methods*. 2014;11(4):417-422. doi:10.1038/nmeth.2869
18. Hekim C, Ilander M, Yan J, et al. Dasatinib changes immune cell profiles concomitant with reduced tumor growth in several murine solid tumor models. *Cancer Immunol Res*. 2017;5:157-169.
19. Ijsselsteijn ME, van der Breggen R, Saraqueta AF, Koning F, de Miranda NF. A 40-marker panel for high dimensional characterization of cancer immune microenvironments by imaging mass cytometry. *Front Immunol*. 2019;10:2534.
20. Khalsa JK, Cheng N, Keegan J, et al. Immune phenotyping of diverse syngeneic murine brain tumors identifies immunologically distinct types. *Nat Commun*. 2020;11:3912.
21. Schapiro D, Jackson HW, Raghuraman S, et al. histoCAT: analysis of cell phenotypes and interactions in multiplex image mass cytometry data. *Nat Methods*. 2017;14:873-876.
22. Carpenter AE, Jones TR, Lamprecht MR, et al. CellProfiler: image analysis software for identifying and quantifying cell phenotypes. *Genome Biol*. 2006;7:R100.
23. Deveney CW, Rand-Luby L, Rutten MJ, et al. Establishment of human colonic epithelial cells in long-term culture. *J Surg Res*. 1996;64: 161-169.
24. Fujii M, Shimokawa M, Date S, et al. A colorectal tumor organoid library demonstrates progressive loss of niche factor requirements during tumorigenesis. *Cell Stem Cell*. 2016;18:827-838.
25. Nearchou IP, Gwyther BM, Georgiakakis ECT, et al. Spatial immune profiling of the colorectal tumor microenvironment predicts good outcome in stage II patients. *npj Digit Med*. 2020;3:7.
26. Westcott PMK, Sacks NJ, Schenkel JM, et al. Low neoantigen expression and poor T-cell priming underlie early immune escape in colorectal cancer. *Nat Cancer*. 2021;2:1071-1085.
27. Tovar Perez JE, Zhang S, Hodgeman W, et al. Epigenetic regulation of major histocompatibility complexes in gastrointestinal malignancies and the potential for clinical interception. *Clin Epigenetics*. 2024;16(1):83.
28. Kobayashi KS, van den Elsen PJ. NLRC5: a key regulator of MHC class I-dependent immune responses. *Nat Rev Immunol*. 2012;12: 813-820.
29. Burr ML, Sparbier CE, Chan KL, et al. An evolutionarily conserved function of polycomb silences the MHC class I antigen presentation pathway and enables immune evasion in cancer. *Cancer Cell*. 2019;36: 385-401.
30. Wang X, Semba T, Manyam GC, et al. EGFR is a master switch between immunosuppressive and immunoactive tumor microenvironment in inflammatory breast cancer. *Sci Adv*. 2022;8:eabn7983.
31. Forssell J, Öberg Å, Henriksson ML, Stenling R, Jung A, Palmqvist R. High macrophage infiltration along the tumor front correlates with improved survival in colon cancer. *Clin Cancer Res*. 2007;13:1472-1479.
32. Kang J-C, Chen J-S, Lee C-H, Chang J-J, Shieh Y-S. Intratumoral macrophage counts correlate with tumor progression in colorectal cancer. *J Surg Oncol*. 2010;102:242-248.
33. Hanahan D, Coussens LM. Accessories to the crime: functions of cells recruited to the tumor microenvironment. *Cancer Cell*. 2012;21: 309-322.
34. Edin S, Wikberg ML, Dahlin AM, et al. The distribution of macrophages with a M1 or M2 phenotype in relation to prognosis and the molecular characteristics of colorectal cancer. *PLoS One*. 2012;7: e47045.
35. Koelzer VH, Canonica K, Dawson H, et al. Phenotyping of tumor-associated macrophages in colorectal cancer: impact on single cell invasion (tumor budding) and clinicopathological outcome. *Onco Targets Ther*. 2015;5:e1106677.
36. Trumpi K, Frenkel N, Peters T, et al. Macrophages induced "budding" in aggressive human colon cancer subtypes by protease-mediated disruption of tight junctions. *Oncotarget*. 2018;9(28):19490-19507. doi: 10.18632/oncotarget.24626
37. Feng Q, Chang W, Mao Y, et al. Tumor-associated macrophages as prognostic and predictive biomarkers for postoperative adjuvant chemotherapy in patients with stage II colon cancer. *Clin Cancer Res*. 2019;25:3896-3907.
38. Yang C, Wei C, Wang S, et al. Elevated $CD163^+/CD68^+$ ratio at tumor invasive front is closely associated with aggressive phenotype and poor prognosis in colorectal cancer. *Int J Biol Sci*. 2019;15: 984-998.
39. Jackaman C, Yeoh TL, Acuil ML, Gardner JK, Nelson DJ. Murine mesothelioma induces locally-proliferating $IL\text{-}10^+TNF\text{-}\alpha^+CD206^-CX3CR1^+$ M3 macrophages that can be selectively depleted by chemotherapy or immunotherapy. *Onco Targets Ther*. 2016;5:e1173299.
40. Kalish S, Lyamina S, Manukhina E, Malyshev Y, Raetskaya A, Malyshev I. M3 macrophages stop division of tumor cells in vitro and extend survival of mice with Ehrlich ascites carcinoma. *Med Sci Monit Basic Res*. 2017;23:8-19.
41. Chávez-Galán L, Olleros ML, Vesin D, Garcia I. Much more than M1 and M2 macrophages, there are also $CD169^+$ and TCR^+ macrophages. *Front Immunol*. 2015;6:263.
42. Poznyak A, Nikiforov N, Starodubova AV, Popkova TV, Orekhov AN. Macrophages and foam cells: brief overview of their roles, linkage, and targeting potential in atherosclerosis. *Biomedicine*. 2021;9:1221.
43. Murray PJ, Allen JE, Biswas SK, et al. Macrophage activation and polarization: nomenclature and experimental guidelines. *Immunity*. 2014;41:14-20.
44. Gurpinar E, Grizzle WE, Piazza GA. NSAIDs inhibit tumorigenesis, but how? *Clin Cancer Res*. 2014;20:1104-1113.
45. Liggett JL, Zhang X, Eling TE, Baek SJ. Anti-tumor activity of non-steroidal anti-inflammatory drugs: cyclooxygenase-independent targets. *Cancer Lett*. 2014;346:217-224.
46. Reyes-Uribe L, Wu W, Gelncik O, et al. Naproxen chemoprevention promotes immune activation in Lynch syndrome colorectal mucosa. *Gut*. 2021;70:555-566.
47. Hardbower DM, Coburn LA, Asim M, et al. Egfr-mediated macrophage activation promotes colitis-associated tumorigenesis. *Oncogene*. 2017;36:3807-3819.
48. Orner GA, Dashwood WM, Blum CA, Diaz GD, Li Q, Dashwood RH. Suppression of tumorigenesis in the Apcmin mouse: down-regulation of β-catenin signaling by a combination of tea plus sulindac. *Carcinogenesis*. 2003;24:263-267.
49. Li N, Xi Y, Tinsley HN, et al. Sulindac selectively inhibits colon tumor cell growth by activating the cGMP/PKG pathway to suppress Wnt/β-catenin signaling. *Mol Cancer Ther*. 2013;12:1848-1859.
50. Yi B, Cheng H, Wyczechowska D, et al. Sulindac modulates the response of proficient MMR colorectal cancer to anti-PD-L1 immunotherapy. *Mol Cancer Ther*. 2021;20:1295-1304.
51. Hu X, Wu L-W, Weng X, Lin N-M, Zhang C. Synergistic antitumor activity of aspirin and erlotinib: inhibition of p38 enhanced aspirin plus erlotinib-induced suppression of metastasis and promoted cancer cell apoptosis. *Oncol Lett*. 2018;16:2715-2724.
52. Monterroza L, Parrilla MM, Samaranayake SG, et al. Tumor-intrinsic enhancer of zeste homolog 2 controls immune cell infiltration, tumor growth, and lung metastasis in a triple-negative breast cancer model. *Int J Mol Sci*. 2024;25(10):5392.
53. Spira A, Yurgelun MB, Alexandrov L, et al. Precancer atlas to drive precision prevention trials. *Cancer Res*. 2017;77:1510-1541.

54. Liu M, Zhong XS, Krishnachaitanya SS, et al. Erlotinib suppresses tumorigenesis in a mouse model of colitis-associated cancer. *Biomed Pharmacother*. 2024;175:116580.

SUPPORTING INFORMATION

Additional supporting information can be found online in the Supporting Information section at the end of this article.

How to cite this article: Tripathi C, Tovar Perez JE, Kapoor S, et al. Antitumor efficacy of intermittent low-dose erlotinib plus sulindac via MHC upregulation and remodeling of the immune cell niche. *Int J Cancer*. 2025;157(2):355-370. doi:10.1002/ijc.35409